Colloids and Surfaces B: Biointerfaces 148 (2016) 270–277

Contents lists available at ScienceDirect

Colloids and Surfaces B: Biointerfaces

journal homepage: www.elsevier.com/locate/colsurfb

Influence of membrane surface charge on adsorption of complement proteins onto supported lipid bilayers

Saziye Yorulmaz[a,b,c], Joshua A. Jackman[a,b], Walter Hunziker[c,d,e], Nam-Joon Cho[a,b,f,*]

[a] School of Materials Science and Engineering, Nanyang Technological University, 50 Nanyang Avenue, 639798, Singapore
[b] Centre for Biomimetic Sensor Science, Nanyang Technological University, 50 Nanyang Drive, 637553, Singapore
[c] Institute of Molecular and Cell Biology, Agency for Science Technology and Research, Singapore
[d] Department of Physiology, Yong Loo Lin School of Medicine, National University of Singapore, 117599, Singapore
[e] Singapore Eye Research Institute, Singapore
[f] School of Chemical and Biomedical Engineering, Nanyang Technological University, 62 Nanyang Drive, 637459, Singapore

ARTICLE INFO

Article history:
Received 17 March 2016
Received in revised form 29 July 2016
Accepted 21 August 2016
Available online 22 August 2016

Keywords:
Biomaterial interfaces
Protein adsorption
Complement activation
Supported lipid bilayer
Quartz crystal microbalance

ABSTRACT

The complement system is an important part of the innate immune response, and there is great interest in understanding how complement proteins interact with lipid membrane interfaces, especially in the context of recognizing foreign particulates (e.g., liposomal nanomedicines). Herein, a supported lipid bilayer platform was employed in order to investigate the effect of membrane surface charge (positive, negative, or neutral) on the adsorption of three complement proteins. Quartz crystal microbalance-dissipation (QCM-D) experiments measured the real-time kinetics and total uptake of protein adsorption onto supported lipid bilayers. The results demonstrate that all three proteins exhibit preferential, mainly irreversible adsorption onto negatively charged lipid bilayers, yet there was also significant variation in total uptake and the relative degree of adsorption onto negatively charged bilayers versus neutral and positively charged bilayers. The total uptake was also observed to strongly depend on the bulk protein concentration. Taken together, our findings contribute to a broader understanding of the factors which influence adsorption of complement proteins onto lipid membranes and offer guidance towards the design of synthetic lipid bilayers with immunocompetent features.

1. Introduction

The complement system is the first line of host defense that responds to pathogenic invaders[1–3] (e.g., bacteria, viruses) and damaged host cells[4–6] (e.g., apoptotic or necrotic cells) by promoting their clearance. A complex and highly orchestrated sequence of complement proteins, typically soluble and cell surface proteins found in extracellular fluids, act in coordinated fashion to mediate a rapid and vital immune response. The initiation of complement activation is a critical first step of recognition and occurs through one of three distinct pathways [7,8]; antibody-antigen interaction on the target surface (*classical pathway*) [9], binding of a mannan-binding lectin (MBL) to terminal sugar molecules on the surface of microorganisms (*lectin pathway*) [10], or nonspecific deposition of complement proteins on the surface of foreign particulates (*alternative pathway*) [11,12].

In contrast to the highly specific initiatory steps involved in the classical and lectin pathways, the alternative pathway of the complement system is continuously and spontaneously activated at a low and regulated level [13]. When a foreign particulate is detected, the level of activation is amplified through the deposition of pattern recognition proteins from the alternative pathway onto the target surface [14,15]. The deposited proteins have multiple functions, including acting as opsonins which facilitate clearance by the reticuloendothelial system (RES) as well as initiators which initiate a proteolytic cascade to generate potent effector molecules that stimulate (*recruit*) immune cells or induce complement-mediated lysis [16–18]. For these reasons, there is great interest in understanding the factors which influence the adsorption of complement proteins onto target surfaces.

While conventional assays to study the complement system focus on measuring hemolysis [19,20] or generation of soluble complement products [21–25], there is growing attention to surface-sensitive measurement approaches to measure the deposition of complement proteins on target surfaces due to their distinct functional properties over generated proteins. In particular,

* Corresponding author at: School of Materials Science and Engineering, Nanyang Technological University, 50 Nanyang Avenue, 639798, Singapore.
E-mail address: njcho@ntu.edu.sg (N.-J. Cho).

http://dx.doi.org/10.1016/j.colsurfb.2016.08.036
0927-7765/

surface-sensitive analytical tools such as ellipsometry, surface plasmon resonance (SPR) and quartz crystal microbalance-dissipation (QCM-D) are popular tools to measure the adsorption of complement proteins in a label-free and real-time measurement format [26,27]. Such measurements are typically performed in one of two ways. The most common option is to incubate a model surface with serum, followed by exchange with an aqueous buffer solution. Then, adsorbed proteins at a model surface are identified by addition of a specific antibody that recognizes a complement protein [27–29]. Antibody binding to the serum treated-surface infers the presence of the deposited complement protein which reveals surface-mediated complement activation [29–31]. To date, this approach has enabled the study of the adsorption of certain complement proteins onto many medically relevant model surfaces such as inorganic substrates [27,32–34], protein-coated substrates [27], polymeric surfaces [35–38] and self-assembled monolayers (SAMs) [39–41]. Another option is to add purified complement proteins and directly monitor their binding to the surface, however, there are few studies in this direction despite the utility of this measurement format for analyzing protein adsorption [42–45]. Indeed, direct measurement of protein adsorption onto target surfaces would be advantageous because, in many previous studies, the C3b pattern recognition protein was the main focus and it was covalently attached to the target surface beforehand in order to monitor its interaction with other complement proteins [46,47]. The covalent attachment of complement proteins to the substrate was generally chosen because it permits efficient use of protein reagents [48–50]. However, this approach prevents monitoring of real-time target recognition through deposition of the complement proteins. Therefore, understanding the factors which influence the noncovalent adsorption of complement proteins onto target surfaces is still an outstanding subject due to its important role in target recognition [40]. Moreover, there has been limited exploration of the deposition of complement proteins in general on more biologically relevant interfaces such as lipid membranes, with only one investigation relating to the deposition of C3 protein on zwitterionic lipid bilayers [51].

Given the scope of lipid membranes involved in triggering complement activation, there is significant potential for investigating how lipid membrane properties influence complement protein deposition. To date, lipid membrane investigations have been principally limited to solution-based liposome systems, as studied in many in vitro and in vivo studies that focus on measuring the generation of complement products [52–59]. In the context of opsonization, these studies have shown that negatively charged liposomes are cleared more rapidly from the circulation through RES uptake due to binding of serum proteins (opsonins) [57,60,61]. Moreover, it is known that both negatively and positively charged liposomes activate the complement system significantly more than neutral liposomes [62,63]. While the functional consequences of membrane surface charge are relatively well understood, the influence of membrane surface charge on the deposition of complement proteins remains to be studied. Indeed, there is growing evidence that the role of electrostatic forces in governing protein adsorption can be complex and the electric dipole of the protein itself should also be considered in terms of its binding affinity and orientation to a target surface [64–69].

The goal of this study is to investigate how membrane surface charge influences the adsorption of three different pattern recognition proteins – C3b, C3 and properdin – onto lipid bilayer membranes. Historically, C3 and C3b proteins are the most widely studied pattern recognition proteins and properdin (Factor P) is a newly identified one [15,70]. In order to achieve this goal, we sought to extend the capabilities of supported lipid bilayers which have been recently employed to study other aspects of the innate immune response, including membrane association of membrane attack complex proteins and inhibition thereof [71,72]. Supported lipid bilayers with positive, neutral or negative surface charges were fabricated by the solvent-assisted lipid bilayer (SALB) method, and the quartz crystal microbalance-dissipation (QCM-D) measurement technique was utilized in order to track protein adsorption in a real-time, label-free format. The membrane surface charge of the supported lipid bilayer was varied based on tuning the lipid composition. Taken together, the findings in this work help to establish a platform to study the adsorption of pattern recognition proteins onto lipid bilayer membranes.

2. Materials and methods

2.1. Protein reagents

Purified human C3, C3b and properdin (Factor P) proteins were purchased from Complement Technology (Tyler, TX). As presented in Table S1 (see in the online version at DOI: http://dx.doi.org/10.1016/j.colsurfb.2016.08.036), C3 is the most abundant complement protein in plasma and has a molar mass of 185 kDa. C3b protein is a 176 kDa fragment of the C3 protein that is obtained through proteolytic conversion. Both C3 and C3b proteins have isoelectric points below 6 and possess negative net charges under neutral pH conditions [73,74]. By contrast, properdin is a much smaller protein with a molar mass of 53 kDa and has an isoelectric point around 9.5 [75–77]; hence, it has a positive net charge under neutral pH conditions. Also, properdin monomers are known to self-associate forming dimers, trimers, and tetramers in the relative portion of 26:54:20 [78–80]. The stock aliquots of complement proteins were prepared in a 10 mM sodium phosphate [pH 7.2] buffer solution with 145 mM NaCl, and were stored at −80 °C until the experiment. Immediately before experiment, the proteins were diluted in a 10 mM Tris [pH 7.5] buffer solution with 150 mM NaCl to the appropriate test concentration.

2.2. Lipid reagents

1,2-dioleoyl-*sn*-*glycero*-3-phosphocholine (DOPC), 1,2-dioleoyl-sn-*glycero*-3-ethylphosphocholine (chloride salt) (DOEPC), 1,2-dioleoyl-3-trimethylammonium-propane (chloride salt) (DOTAP) and 1-palmitoyl-2-oleoyl-*sn*-glycero-3-phospho-(1′-*rac*-glycerol) (sodium salt) (POPG) were obtained in lyophilized powder form from Avanti Polar Lipids (Alabaster, AL). The lipid powders were stored at -20 °C until experiment and were then diluted in the appropriate organic solvent. The chemical structures of the phospholipid molecules are presented in Fig. 1. The DOEPC and DOTAP lipids are positively charged lipids while POPG is a negatively charged lipid and DOPC is a zwitterionic lipid.

2.3. Quartz crystal microbalance with dissipation (QCM-D) monitoring

A Q-Sense E4 instrument (Q-sense AB, Gothenburg, Sweden) was utilized in order to monitor lipid and protein adsorption processes by tracking changes in resonance frequency and energy dissipation of a silicon oxide-coated quartz crystal (model no. QSX303) as a function of time. The QCM-D measurement data were collected at the 3rd, 5th, 7th, 9th, and 11th odd overtones, and the reported QCM-D data were all obtained at the 5th overtone and normalized accordingly ($\Delta f_{n=5}/5$). Immediately before the experiment, the QCM-D sensor substrates were sequentially rinsed with 2% SDS, water, and ethanol followed by drying with nitrogen gas. The substrates were then subjected to oxygen plasma treatment (Harrick Plasma, Ithaca, NY) at the maximum radiofrequency (RF) power. All QCM-D measurements were conducted under continuous flow conditions, with the flow rate defined as 100 μL/min for

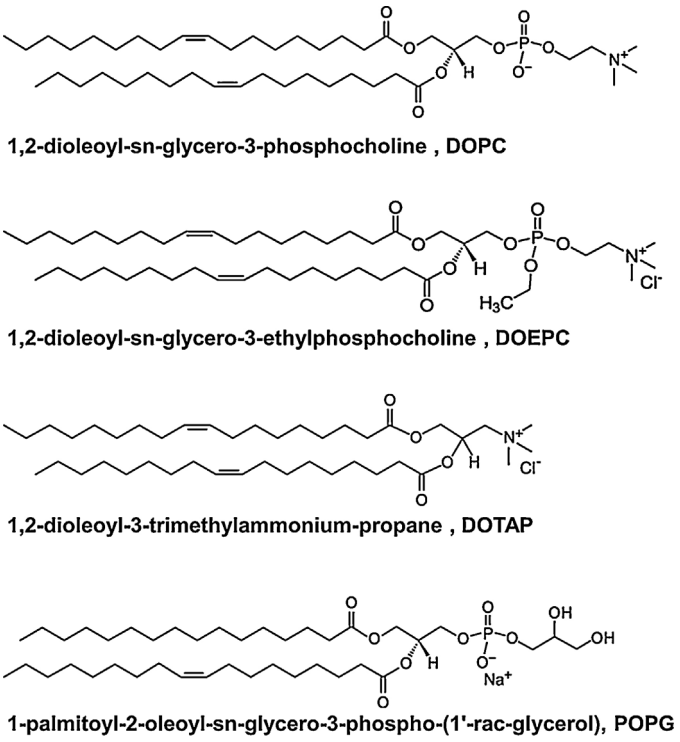

Fig. 1. Chemical structure of phospholipid molecules used in this study. The net charges correspond to the state under neutral pH conditions.

all of the steps in the bilayer formation and washing processes and 41.8 μL/min for the protein addition as controlled by a Reglo Digital peristaltic pump (Ismatec, Glattbrugg, Switzerland). The temperature of the flow cell was fixed at 24.0 ± 0.5 °C. In order to estimate the molecular ratio of adsorbed proteins, the Sauerbrey model was applied in order to convert frequency shifts into mass density values as follows:

$$\Delta m = -C\frac{\Delta f_n}{n},$$

where Δm is the adsorbate mass, C is the proportionality constant (17.7 ng/cm^2), Δf is the frequency shift, and n is the odd overtone number of the resonance frequency [81].

2.4. Supported lipid bilayer formation

The solvent-assisted lipid bilayer (SALB) formation method [82,83] was employed in order to prepare supported lipid bilayers, as previously demonstrated for charged lipid compositions [84]. For SALB experiments, the DOPC, DOEPC and DOTAP lipid powders were dissolved in isopropanol at a stock concentration of 10 mg/mL. The POPG lipid powder was dissolved in ethanol at a concentration of 5 mg/mL and incubated around 40 °C in order to promote solubilization. Before the experiment, the lipid solutions were mixed to the desired molar ratio and diluted in isopropanol to a final concentration of 0.5 mg/mL. As part of the SALB experimental protocol, a measurement baseline was first recorded in aqueous buffer solution (10 mM Tris [pH 7.5] with 150 mM NaCl) (Step 1), followed by exchange with isopropanol solution (Step 2). Then, 0.5 mg/mL lipid in isopropanol was deposited onto the substrate (Step 3), and incubated for approximately 10 min before a solvent-exchange step was performed as aqueous buffer solution was reintroduced leading to bilayer formation (Step 4). After bilayer formation, 0.1 mg/mL BSA was added (Step 5) in order to verify the completeness of bilayer formation.

2.5. Vesicle preparation

Lipid powders were suspended in chloroform and then mixed to the desired molar ratio. A dried lipid film was formed by evaporating the chloroform upon exposure to a gentle stream of nitrogen gas. The dried lipid films were then placed in a vacuum desiccator overnight in order to remove residual chloroform. After storage, the dried lipid films were hydrated in 10 mM Tris [pH 7.5] buffer solution with 150 mM NaCl and subjected to vortexing. The resulting vesicle suspension was extruded a minimum of 13 times through a track-etched polycarbonate membrane with 200 nm diameter pores by using a Mini Extruder apparatus (Avanti Polar Lipids).

2.6. Zeta potential measurements

The electrophoretic mobility of vesicles in solution was determined by laser doppler velocimetry and phase analysis light scattering measurements. A Malvern Zetasizer Nano ZS ZEN 3600 (Malvern Instruments Inc, UK) with a 633 nm wavelength laser was used for all measurements. The vesicle samples were diluted in a 10:1 voltric ratio with 10 mM Tris [pH 7.5] buffer solution with 10 mM NaCl. The temperature of all experiments was set at 24 °C.

2.7. Statistical analysis

Measurements were conducted in triplicate and the results are expressed as mean ± standard deviation (SD) of the mean. Statistical analysis was performed using the OriginPro 9 software program (OriginLab Corporation, Northampton, MA). One way analysis of variance (ANOVA), followed by the Bonferroni test was conducted and a P value of less than 0.05 was considered to be statistically significant.

3. Results and discussion

3.1. Supported lipid bilayer fabrication

In order to determine how membrane surface charge affects the adsorption behavior of C3, C3b and properdin proteins onto lipid membrane surfaces, we first established a supported lipid bilayer (SLB) platform on a silicon dioxide substrate by employing the solvent-assisted lipid bilayer (SALB) formation protocol as outlined above (Fig. 2a). The SLB fabrication process was followed in real-time by QCM-D measurement analysis in order to characterize the mass and viscoelastic properties of the adlayer on the basis of resonance frequency (Δf) and energy dissipation (ΔD) shifts, respectively. Representative QCM-D sensorgrams are presented in Fig. 2b and SLB formation occurred for all lipid compositions, as indicated by Δf and ΔD shifts of -25.6 ± 2.0 Hz and $0.6 \pm 0.3 \times 10^{-6}$, respectively, which agree with previously reported values [71,82]. The lipid composition was varied in order to create a negatively or positively charged or neutral membrane surface. The chosen zwitterionic lipid was DOPC; for charged lipid compositions, 70 mol% DOPC was mixed with 30 mol% DOEPC or DOTAP for positively charged SLBs or 30 mol% POPG for negatively charged SLBs. The surface charge of the resultant SLBs was estimated by preparing lipid vesicles of equivalent lipid membrane composition for zeta potential measurements (Fig. S1 in the online version at DOI: http://dx.doi.org/10.1016/j.colsurfb.2016.08.036). The zeta potential of the negatively charged 70/30 DOPC/POPG vesicles was -50.4 ± 2.9 mV while the zwitterionic DOPC vesicles had a zeta potential of -3.9 ± 1.3 mV. On the other hand, the zeta potential values of the positively charged 70/30 DOPC/DOEPC and 70/30 DOPC/DOTAP vesicles were 59.5 ± 2.6 mV and 25.2 ± 3 mV, respectively. Hence, this range of lipid compositions is suitable for preparing SLBs with variable surface charges.

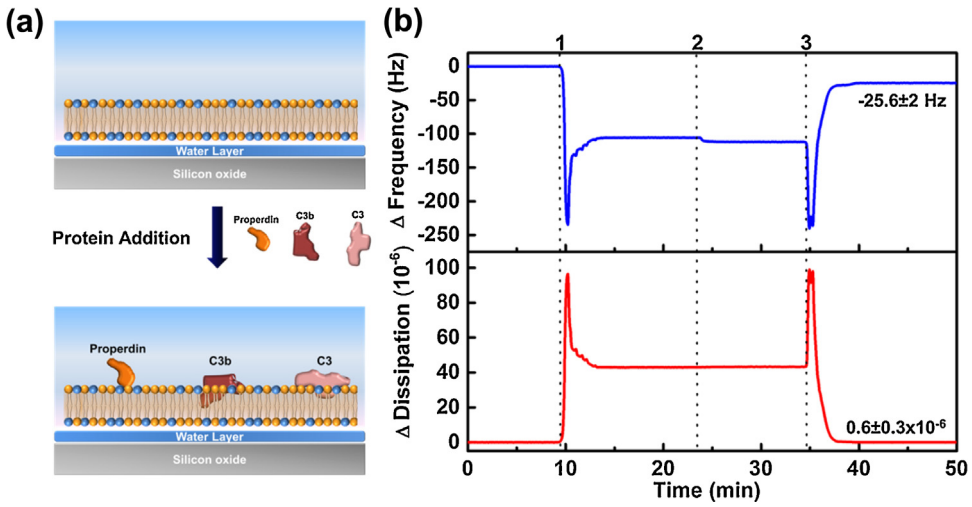

Fig. 2. Design of supported lipid bilayer platform to investigate membrane association of pattern recognition proteins. (a) Schematic of supported lipid bilayer platform and protein binding to charged lipid bilayers. (b) Quartz crystal microbalance-dissipation (QCM-D) measurements provide a label-free measurement technique in order to measure changes in resonance frequency and energy dissipation upon formation of supported lipid bilayer via the SALB fabrication method. The numbers denote the injection of (1) isopropanol, (2) lipid in isopropanol, and (3) buffer, respectively.

After SLB formation, 0.1 mg/mL bovine serum albumin (BSA) was added to bare and SLB-coated silicon dioxide substrates. Considering that zwitterionic SLBs are known to inhibit BSA adsorption, the degree of SLB coverage on the silicon dioxide substrate was estimated to be >90% complete [85]. The BSA blocking step also passivated any exposed areas on the silicon dioxide substrate, ensuring that subsequent detection of complement protein adsorption occurred only on the lipid bilayer surface. Following the blocking step, the QCM-D measurement signals were normalized and the baseline signals were reestablished in order to focus on membrane association of the pattern recognition proteins. After stable baseline signals were recorded for 10 min, 500 nM of the chosen protein - purified human C3, C3b or properdin - was injected under continuous flow conditions.

3.2. Membrane association of complement proteins

3.2.1. C3 protein

The QCM-D sensorgrams of the Δf and ΔD shifts for 500 nM C3 protein adsorption onto different-charge SLB platforms are presented in Fig. 3a and b, respectively. Significantly higher protein adsorption was observed to negatively charged SLBs, with final Δf shifts of -16.2 ± 1.1 Hz. By contrast, the final Δf shifts were -3.5 ± 0.8 Hz for protein adsorption onto positively charged 70/30 DOPC/DOEPC SLBs and there were only minor shifts around -1 Hz on neutral and positively charged 70/30 DOPC/DOTAP SLBs. In all cases, protein adsorption led to only minor ΔD shifts, indicating that membrane-associated C3 protein possesses a rigid conformation. Based on repeated experiments, it was determined that C3 adsorption onto negatively charged SLBs is statistically significant compared to the cases on other SLBs (Fig. 3c). Considering the negative net charge of C3 protein under the tested conditions [74], this finding suggests that there is a positively charged domain within the C3 protein which is involved in membrane association onto negatively charged SLBs [22,44]. Beyond net charge, the dipole moment of the protein is another important factor in the context of how electrostatic forces can mediate C3 adsorption onto both negatively and positively charged SLBs [65,67,68]. Indeed, while C3 adsorption was greatest onto negatively charged SLBs, moderate C3 binding was also observed onto positively charged SLBs (cf. Fig. 3C). Of note, C3 adsorption onto 70/30 DOPC/DOEPC SLBs was greater than onto 70/30 DOPC/DOTAP SLBs, which is consistent with attractive electrostatic forces modulating protein adsorption because 70/30 DOPC/DOEPC SLBs have more appreciable positive surface charge than 70/30 DOPC/DOTAP SLBs (cf. Fig. S1 see in the online version at DOI: http://dx.doi.org/10.1016/j.colsurfb.2016.08.036).

Following our observation that C3 protein adsorption is most appreciable on negatively charged SLBs, we further investigated the effect of bulk protein concentration on the adsorption uptake on negatively charged SLBs. As proteins are relatively large macromolecules, the rate of protein uptake is limited by their diffusion in bulk solution, which in turn depends on the bulk protein concentration [86]. With increasing protein concentration, the adsorption kinetics had a shorter time scale and a larger final Δf shift was observed across the test range (63–500 nM C3 protein), as shown in Fig. 3d and e. The final Δf shifts ranged from -2.5 ± 0.6 Hz at 63 nM protein to -16.2 ± 1.1 Hz at 500 nM protein. There were negligible ΔD shifts always below 0.3×10^{-6} in all cases. There was a clear dependence of the absolute frequency shift due to bound C3 protein as a function of the bulk protein concentration (Fig. 3f). This trend supports that the rate of protein adsorption is diffusion-limited up to a relatively large uptake. Taken together, the results indicate that C3 protein moderately prefers adsorption onto negatively charged SLBs which occurs in a protein concentration-dependent manner.

3.2.2. C3b protein

The QCM-D sensorgrams of the Δf and ΔD shifts for 500 nM C3b protein adsorption onto different-charge SLB platforms are presented in Fig. 4a and b, respectively. While C3b still exhibited greatest adsorption onto negatively charged SLBs, its binding preference for negatively charged SLBs over other SLBs was markedly lower than that of C3 protein. The final Δf shift on the negatively charged SLB was −4.5 ± 1.4 Hz, versus final Δf shifts around −1 to −3 Hz on the neutral and positively charged SLBs. Again, the final ΔD shifts were nearly negligible in all cases, suggesting a rigid conformation of membrane-associated C3b protein. Comparatively, the extent of C3b protein adsorption mirrored the results obtained for C3 protein adsorption onto neutral and positively charged SLBs, with the same binding preference for DOPC/DOEPC 70/30 SLBs over DOPC/DOTAP 70/30 SLBs arising from stronger electrostatic attraction (Fig. 4c). Furthermore, while tempered, the binding preference for negatively charged SLBs is consistent with the presence of a cationic patch near the purported membrane association domain of C3b protein [73,87]. Further experiments on negatively charged

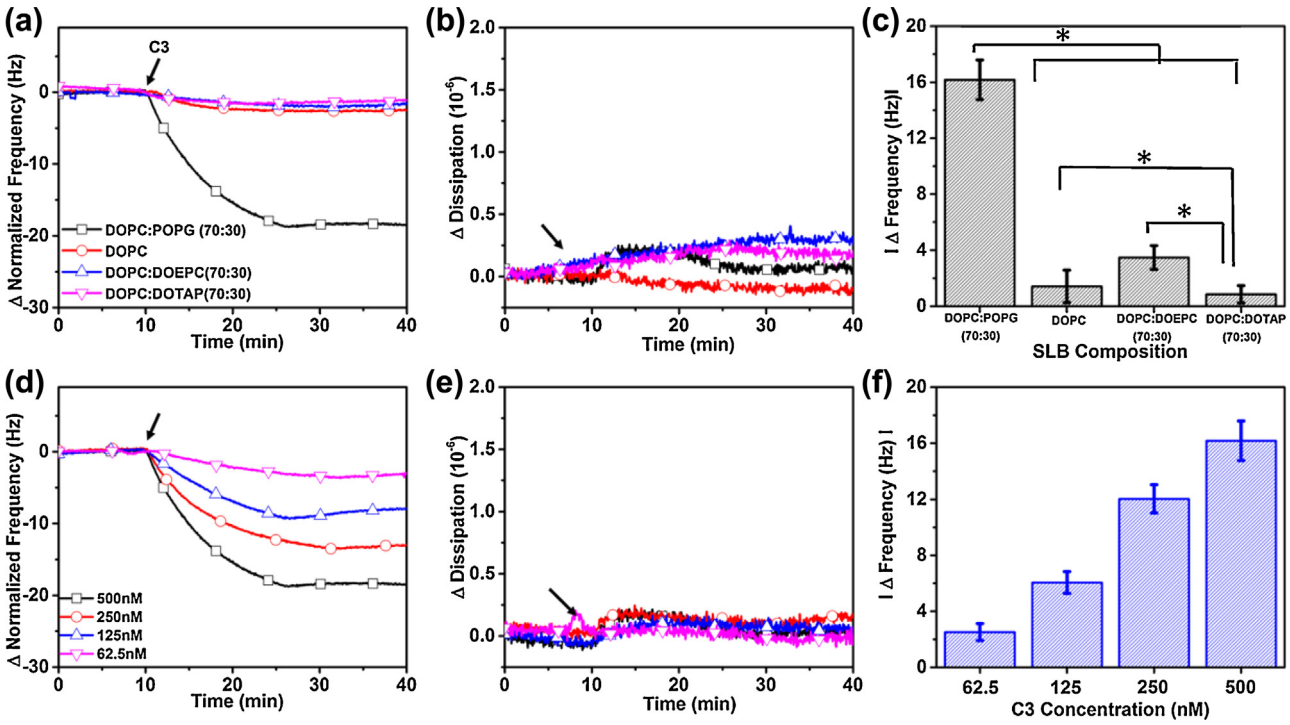

Fig. 3. Influence of membrane surface charge on C3 protein adsorption. After SLB formation, the QCM-D Δf and ΔD shifts were normalized to zero and then 500 nM C3 protein was added after 10 min baseline. Changes in (a) normalized frequency and (b) energy dissipation are presented as a function of time. Arrow indicates protein injection. (c) Changes in absolute frequency shifts on different SLB platforms. Changes in (d) normalized frequency and **(e)** energy dissipation as function of time for C3 protein adsorption onto 70/30 DOPC/POPG supported lipid bilayer at various bulk protein concentrations. (f) Changes in absolute frequency shifts as a function of bulk protein concentration. Error bars indicate the average + standard deviations of three independent ($n = 3$) measurements.

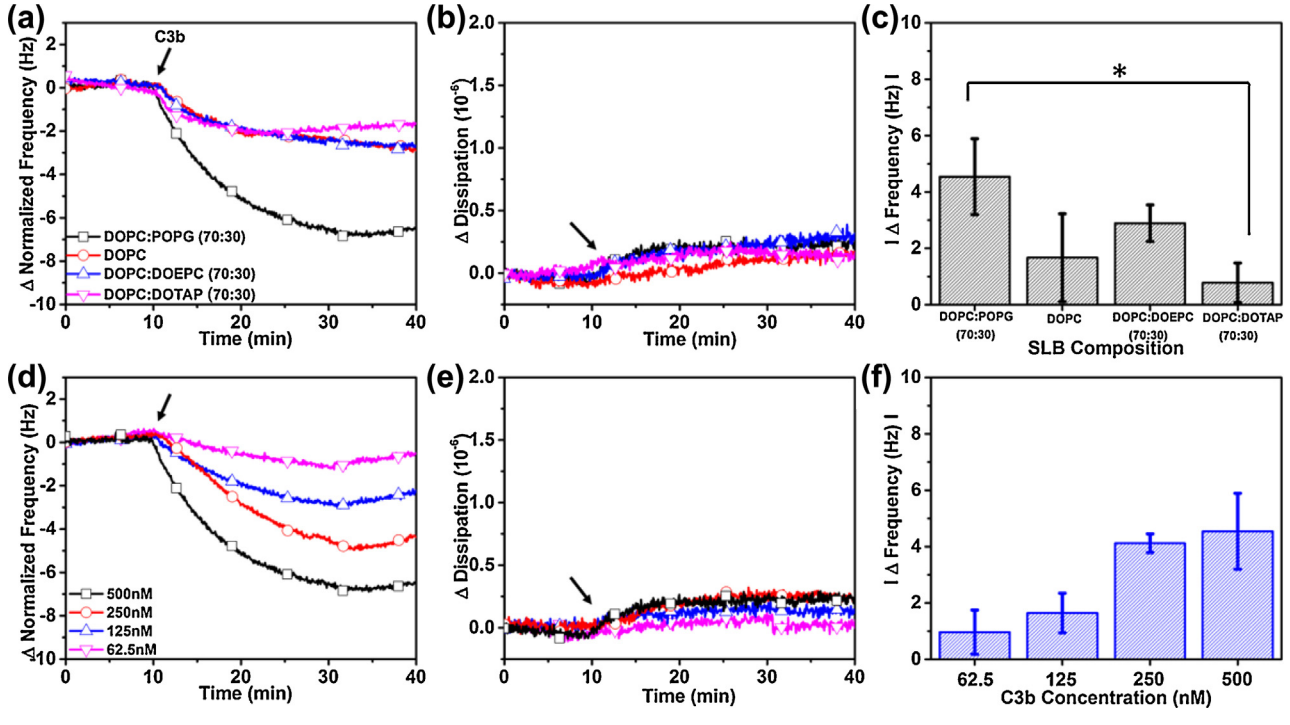

Fig. 4. Influence of membrane surface charge on C3b protein adsorption. After SLB formation, the QCM-D Δf and ΔD shifts were normalized to zero and then 500 nM C3b protein was added after 10 min baseline. Changes in (a) normalized frequency and (b) energy dissipation are presented as a function of time. Arrow indicates protein injection. (c) Changes in absolute frequency shifts upon association of the C3b protein on different SLB platforms. Changes in (d) normalized frequency and (e) energy dissipation as function of time for C3b protein adsorption onto 70/30 DOPC/POPG supported lipid bilayer at various bulk protein concentrations. (f) Changes in the absolute frequency shifts on negatively charged SLBs as a function of bulk C3b protein concentration. Error bars indicate the average + standard deviations of three independent ($n = 3$) measurements.

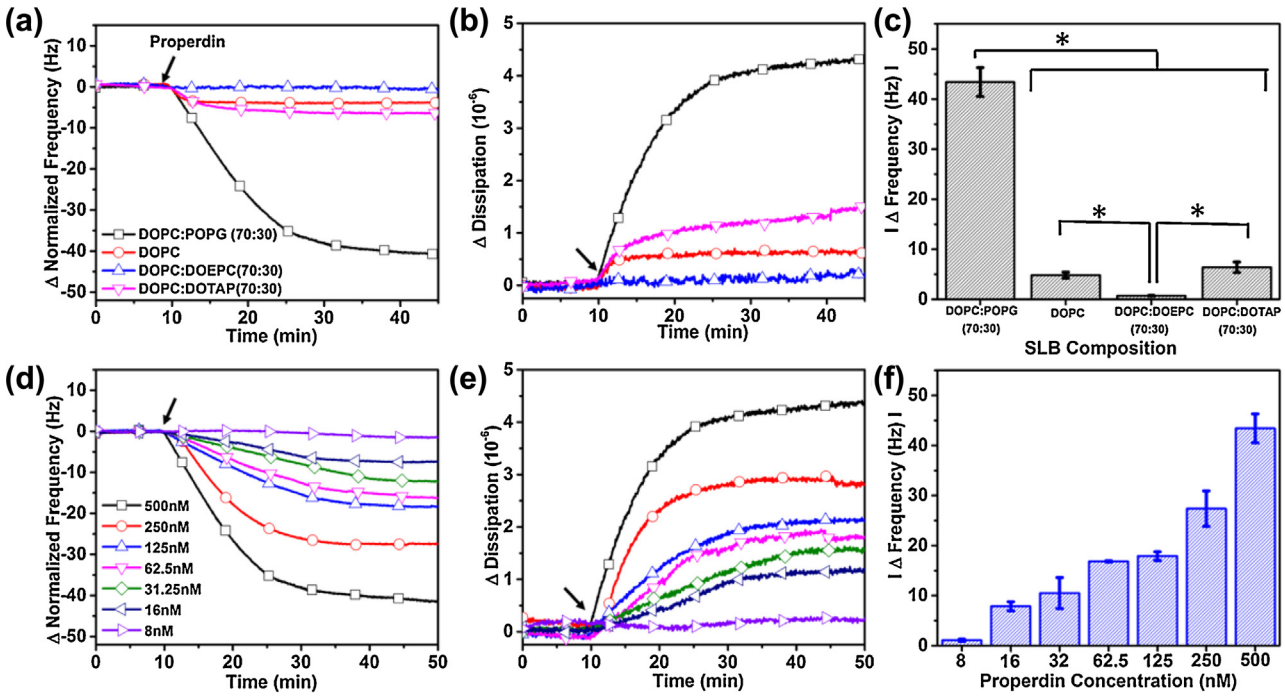

Fig. 5. Influence of membrane surface charge on properdin adsorption. After SLB formation, the QCM-D Δf and ΔD shifts were normalized to zero and then 500 nM properdin was added after 10 min baseline. Changes in (a) normalized frequency and (b) energy dissipation are presented as a function of time. Arrow indicates protein injection. (c) Changes in absolute frequency shifts due to adsorption of properdin on different SLB platforms. Changes in (d) normalized frequency and (e) energy dissipation as function of time for properdin adsorption onto 70/30 DOPC/POPG supported lipid bilayer at various bulk protein concentrations. (f) Changes in absolute frequency as a function of bulk properdin protein concentration. Error bars indicate the average + standard deviations of three independent ($n = 3$) measurements.

SLBs showed that the extent of C3b protein uptake and corresponding adsorption kinetics varied with the bulk protein concentration, as indicated by the Δf and ΔD shifts (Fig. 4d and e). Likewise, the absolute frequency shifts upon association of C3b varied with the bulk protein concentration and support that C3b protein adsorption is diffusion-limited (Fig. 4f). Overall, the results indicate that C3b protein preferentially binds to negatively charged SLBs, albeit the preference is weaker than that of C3 protein and the total protein uptake is relatively low under all tested conditions.

3.2.3. Properdin

The QCM-D sensorgrams of the Δf and ΔD shifts for 500 nM properdin adsorption onto different-charge SLB platforms are presented in Fig. 5a and b, respectively. Compared to C3 and C3b proteins, properdin exhibited prodigious adsorption onto negatively charged SLBs with a final Δf shift of -43.4 ± 2.9 Hz. Interestingly, a significant final ΔD shift of $4.4 \pm 0.6 \times 10^{-6}$ was also recorded which supports that membrane-associated properdin has viscoelastic character. Such behavior is likely due to the attachment of protein oligomers as properdin is known to form low-order aggregates (2–4 monomers) in solution [79,80]. On the other hand, properdin adsorption onto the other tested SLBs was tempered yet still appreciable. There was negligible protein adsorption onto 70/30 DOPC/DOEPC SLBs whereas adsorption onto 70/30 DOPC/DOTAP SLBs led to Δf and ΔD shifts of -6.4 ± 1.1 Hz and $1.2 \pm 0.2 \times 10^{-6}$, respectively. Also, properdin binding to neutral DOPC SLBs led to Δf and ΔD shifts of -4.9 ± 0.6 Hz and $0.6 \pm 0.2 \times 10^{-6}$, respectively. Hence, there was moderate binding to both DOPC and 70/30 DOPC/DOTAP SLBs, whereas there was significantly less binding to 70/30 DOPC/DOEPC SLBs, as indicated in Fig. 5c. Taking into account that properdin is highly positively charged, this finding is consistent with the fact that 70/30 DOPC/DOEPC SLBs have greater positive surface charge than 70/30 DOPC/DOTAP SLBs and hence properdin does not bind to 70/30 DOPC/DOEPC SLBs due to repulsive electrostatic forces. Furthermore, the absolute frequency shift onto negatively charged SLBs due to adsorption of properdin was seven-fold higher than to the other SLBs indicating high selectivity on the basis of membrane surface charge. Therefore, membrane association of properdin to negatively charged SLBs was probed as a function of bulk protein concentration. The final Δf and ΔD shifts are presented in Fig. 5d and e, respectively. Protein binding was detectable down to 8 nM concentration and both measurement signals indicated concentration-dependent behavior. The absolute frequency shifts varied by more than 40-fold across the tested concentration range (Fig. 5f). The data indicates that properdin demonstrates strongly preferential adsorption onto negatively charged SLBs with a bound state that exhibits viscoelastic character, supporting that the protein binds in an oligomeric state [88].

3.3. Comparison of membrane association of C3, C3b, and properdin

In order to compare noncovalent membrane association of the different proteins, Table 1 presents the final frequency and dissipation shifts which were obtained under identical experimental conditions in each experimental set. The QCM-D measurement results indicate that membrane association depends on membrane surface charge and the greatest adsorption was observed on negatively charged SLBs for all tested proteins. Interestingly, C3 and its conformationally distinct C3b subunit exhibit striking differences in total protein uptake considering the nearly equivalent molar masses of the two proteins. C3 protein adsorption to negatively charged SLBs was almost four-times greater than that of C3b protein. The main difference between C3 and C3b is the missing C3a subunit which is released through C3 cleavage. Of note, C3a is highly cationic peptide with an isoelectric point of 9.5 [76,77].

To further understand the basis for the different binding preferences of C3 and C3b proteins, we conducted additional membrane binding experiments with C3a peptide (Fig. S2 see in the online

Table 1
QCM- D measurement response at the equilibrium state of protein adsorption on different SLBs.

SLBs Proteins	DOPC		DOPC/DOTAP (70/30)		DOPC/DOEPC (70/30)		DOPC/POPG (70/30)	
	Frequency (Hz)	Dissipation (10^{-6})	Frequency (Hz)	Dissipation (10^{-6})	Frequency (Hz)	Dissipation (10^{-6})	Frequency (Hz)	Dissipation (10^{-6})
C3	-1.42 ± 1.16	0.85 ± 0.06	-0.85 ± 0.62	0.20 ± 0.26	-3.48 ± 0.84	0.49 ± 0.25	-16.17 ± 1.14	0.24 ± 0.20
C3b	-1.67 ± 1.56	0.13 ± 0.06	-0.78 ± 0.70	0.24 ± 0.17	-2.89 ± 0.64	0.33 ± 0.12	-4.54 ± 1.35	0.21 ± 0.11
Properdin	-4.86 ± 0.60	0.57 ± 0.15	-6.40 ± 1.06	1.28 ± 0.24	-0.70 ± 0.05	0.08 ± 0.03	-43.40 ± 2.89	4.43 ± 0.59

version at DOI: http://dx.doi.org/10.1016/j.colsurfb.2016.08.036). Following SLB fabrication as described above, 3 μM C3a peptide was added to the SLB platforms in order to probe membrane association. The QCM-D measurement results indicated that the C3a peptide preferentially adsorbed onto negatively charged SLBs with final Δf shifts around −4 Hz. By contrast, markedly less C3a peptide adsorption was observed onto neutral SLBs with final Δf shifts around −1.5 Hz and there was negligible adsorption onto positively charged SLBs. This finding supports that the positively charged C3a domain is important for promoting C3 membrane association on negatively charged SLBs, i.e., likely as a consequence of attractive electrostatic interactions.

Hence, our findings support that the C3a domain plays an important role in modulating membrane association of C3 protein to negatively charged SLBs, and this difference helps to explain why C3 display high specificity for negatively charged membrane compositions while C3b has weaker discrimination for membrane surface charge. On the other hand, properdin is much smaller yet exhibited more appreciable adsorption with high preference for negatively charged membrane compositions, likely due to its highly positive surface charge and tendency to oligomerize. The corresponding high energy dissipation shifts for properdin adsorption support that it maintains a membrane-associated oligomeric state which may enable its reported multifunctional capabilities.

4. Conclusion

Herein, we have investigated how membrane surface charge regulates the adsorption properties of pattern recognition proteins implicated in the alternative pathway of complement activation. Using the QCM-D measurement technique, the adsorption of three different proteins - C3, C3b and properdin - to charged supported lipid bilayers was investigated. It was identified that all three proteins prefer adsorption onto negatively charged supported lipid bilayers, with variable charge selectivity over the other tested membrane compositions. There were significant differences in the specific details of protein adsorption for each tested protein, including total uptake and membrane charge selectivity. The observed trends in protein adsorption also correlate well with the known trends in RES clearance arising through opsonization. Collectively, these findings improve our knowledge of the biointerfacial science of complement activation, and provide guidelines for designing biomimetic lipid membrane coatings with immunocompetent properties.

Acknowledgments

This work was supported by the National Research Foundation grant NRF-NRFF2011-01, the National Medical Research Council grant NMRC/CBRG/0005/2012, and the A*STAR-NHG-NTU Skin Research Grant (SRG/14028) to N.J.C

Reference:

[1] L.A. Trouw, M.R. Daha, Immunol. Lett. 138 (2011) 35–37.
[2] K.A. Joiner, Annu. Rev. Microbiol. 42 (1988) 201–230.
[3] R.L. Hirsch, Microbiol. Rev. 46 (1982) 71.
[4] P. Gasque, Mol. Immunol. 41 (2004) 1089–1098.
[5] A.J. Nauta, M.R. Daha, C. van Kooten, A. Roos, Trends Immunol. 24 (2003) 148–154.
[6] N.S. Merle, R. Noe, L. Halbwachs-Mecarelli, V. Fremeaux-Bacchi, L.T. Roumenina, Front. Immunol. 6 (2015) 257.
[7] M. Walport, N. Engl. J. Med. 344 (2001) 1058–1066.
[8] N. Merle, S.E. Church, V. Fremeaux-Bacchi, L.T. Roumenina, Front. Immunol. 6 (2015) 262.
[9] K. Reid, The Complement System, Springer, Verlag, Heidelberg, 1998, pp. 68–92.
[10] T. Fujita, M. Matsushita, Y. Endo, Immunol. Rev. 198 (2004) 185–202.
[11] M. Pangburn, Complement. Syst. 93 (1998).
[12] S. Law, R. Levine, Proc. Natl. Acad. Sci. 74 (1977) 2701–2705.
[13] D. Ricklin, J.D. Lambris, Nat. Biotechnol. 25 (2007) 1265–1275.
[14] P.F. Zipfel, M. Mihlan, C. Skerka, Current Topics in Innate Immunity, Springer, 2007, pp. 80–92.
[15] C. Kemper, J.P. Atkinson, D.E. Hourcade, Annu. Rev. Immunol. 28 (2009) 131–155.
[16] R.B. Sim, R. Wallis, Nat. Nanotechnol. 6 (2011) 80–81.
[17] T. Fujita, Y. Endo, M. Nonaka, Mol. Immunol. 41 (2004) 103–111.
[18] X. Yan, G.L. Scherphof, J.A. Kamps, J. Liposome Res. 15 (2005) 109–139.
[19] T.D. Jaskowski, T.B. Martins, C.M. Litwin, H.R. Hill, Clin. Diagn. Lab. Immunol. 6 (1999) 137–139.
[20] T.E. Mollnes, T.S. Jokiranta, L. Truedsson, B. Nilsson, S.R. de Cordoba, M. Kirschfink, Mol. Immunol. 44 (2007) 3838–3849.
[21] A. Meerasa, J.G. Huang, F.X. Gu, Curr. Drug. Deliv. 8 (2011) 290–298.
[22] J. Andersson, R. Larsson, R. Richter, K.N. Ekdahl, B. Nilsson, Biomaterials 22 (2001) 2435–2443.
[23] M. Berger, B. Broxup, M. Sefton, J. Mater. Sci. Mater. Med. 5 (1994) 622–627.
[24] N.R. Cooper, G.R. Nemerow, J.T. Mayes, Springer Semin. Immunopathol, Springer, 1983, pp. 195–212.
[25] J. Wetterö, A. Askendal, T. Bengtsson, P. Tengvall, Biomaterials 23 (2002) 981–991.
[26] P. Tengvall, I. Lundström, B. Liedberg, Biomaterials 19 (1998) 407–422.
[27] A. Sellborn, M. Andersson, C. Fant, C. Gretzer, H. Elwing, Colloids Surf. B Biointerfaces 27 (2003) 295–301.
[28] B. Walivaara, A. Askendal, A. Krozer, I. Lundstrom, P. Tengvall, J. Biomater. Sci. Polym. Ed. 8 (1997) 49–62.
[29] P. Tengvall, A. Askendal, I. Lundström, Biomaterials 19 (1998) 935–940.
[30] S. Arvidsson, A. Askendal, P. Tengvall, Biomaterials 28 (2007) 1346–1354.
[31] P. Tengvall, A. Askendal, J. Biomed. Mater. Res. 57 (2001) 285–290.
[32] A. Sellborn, M. Andersson, J. Hedlund, J. Andersson, M. Berglin, H. Elwing, Mol. Immunol. 42 (2005) 569–574.
[33] H. Elwing, B. Ivarsson, I. Lundstrom, Eur. J. Biochem. 156 (1986) 359–365.
[34] L. Liu, H. Elwing, J. Biomed. Mater. Res. 28 (1994) 767–773.
[35] M. Andersson, J. Andersson, A. Sellborn, M. Berglin, B. Nilsson, H. Elwing, Biosens. Bioelectron. 21 (2005) 79–86.
[36] M. Berglin, M. Andersson, A. Sellborn, H. Elwing, Biomaterials 25 (2004) 4581–4590.
[37] Y. Arima, M. Kawagoe, M. Toda, H. Iwata, ACS Appl. Mater. Interfaces 1 (2009) 2400–2407.
[38] M. Toda, Y. Arima, H. Iwata, Acta Biomater. 6 (2010) 2642–2649.
[39] M. Toda, H. Iwata, ACS Appl. Mater. Interfaces 2 (2010) 1107–1113.
[40] I. Hirata, Y. Hioki, M. Toda, T. Kitazawa, Y. Murakami, E. Kitano, H. Kitamura, Y. Ikada, H. Iwata, J. Biomed. Mater. Res. A 66 (2003) 669–676.
[41] M. Toda, T. Kitazawa, I. Hirata, Y. Hirano, H. Iwata, Biomaterials 29 (2008) 407–417.
[42] J. Andersson, K.N. Ekdahl, R. Larsson, U.R. Nilsson, B. Nilsson, J. Immunol. 168 (2002) 5786–5791.
[43] M. Malmsten, B. Lassen, J. Westin, C.-G. Gölander, R. Larsson, U.R. Nilsson, J. Colloid Interface Sci. 179 (1996) 163–172.
[44] M. Malmsten, B. Lassen, J.M. Van Alstine, U.R. Nilsson, J. Colloid Interface Sci. 178 (1996) 123–134.
[45] H. Elwing, B. Nilsson, K.-E. Svensson, A. Askendahl, U.R. Nilsson, I. Lundström, J. Colloid Interface Sci. 125 (1988) 139–145.
[46] T.S. Jokiranta, J. Westin, U.R. Nilsson, B. Nilsson, J. Hellwage, S. Löfås, D.L. Gordon, K.N. Ekdahl, S. Meri, Int. Immunopharmacol. 1 (2001) 495–506.
[47] S. Law, A.W. Dodds, Protein Sci. 6 (1997) 263–274.
[48] B. Nilsson, R. Larsson, J. Hong, G. Elgue, K.N. Ekdahl, A. Sahu, J.D. Lambris, Blood 92 (1998) 1661–1667.
[49] C.L. Harris, R.J. Abbott, R.A. Smith, B.P. Morgan, S.M. Lea, J. Biol. Chem. 280 (2005) 2569–2578.
[50] D.E. Hourcade, J. Biol. Chem. 281 (2006) 2128–2132.

[51] Y. Klapper, O.A. Hamad, Y. Teramura, G. Leneweit, G.U. Nienhaus, D. Ricklin, J.D. Lambris, K.N. Ekdahl, B. Nilsson, Biomaterials 35 (2014) 3688–3696.
[52] J. Szebeni, F. Muggia, A. Gabizon, Y. Barenholz, Adv. Drug Deliv. Rev. 63 (2011) 1020–1030.
[53] A. Chonn, P. Cullis, D. Devine, J. Immunol, (1991) 4234–4241.
[54] J. Szebeni, S.M. Moghimi, J. Liposome Res. 19 (2009) 85–90.
[55] T. Ishida, H. Harashima, H. Kiwada, Biosci. Rep. 22 (2002) 197–224.
[56] S.M. Moghimi, I. Hamad, J. Liposome Res. 18 (2008) 195–209.
[57] D.V. Devine, K. Wong, K. Serrano, A. Chonn, P.R. Cullis, Biochim. Biophys. Acta Biomembr. 1191 (1994) 43–51.
[58] M.L. Immordino, F. Dosio, L. Cattel, Int. J. Nanomed. 1 (2006) 297.
[59] C.M. Cunningham, M. Kingzette, R.L. Richards, C.R. Alving, T.F. Lint, H. Gewurz, J. Immunol, (1979) 1237–1242.
[60] K. Nishikawa, H. Arai, K. Inoue, J. Biol Chem. 265 (1990) 5226–5231.
[61] R. Juliano, D. Stamp, Biochem. Biophys. Res. Commun. 63 (1975) 651–658.
[62] J. Marjan, Z. Xie, D.V. Devine, Biochim. Biophys. Acta Biomembr. 1192 (1994) 35–44.
[63] A.J. Bradley, D.V. Devine, S.M. Ansell, J. Janzen, D.E. Brooks, Arch. Biochem. Biophys. 357 (1998) 185–194.
[64] Y. Xie, J. Zhou, S. Jiang, J. Chem. Phys. 132 (2010) 065101.
[65] J. Liu, C. Liao, J. Zhou, Langmuir 29 (2013) 11366–11374.
[66] G. Yu, J. Liu, J. Zhou, J. Phys. Chem. B 118 (2014) 4451–4460.
[67] C. Peng, J. Liu, D. Zhao, J. Zhou, Langmuir 30 (2014) 11401–11411.
[68] J. Liu, G. Yu, J. Zhou, Chem. Eng. Technol. 121 (2015) 331–339.
[69] D. Zhao, C. Peng, J. Zhou, Phys. Chem. Chem. Phys. 17 (2015) 840–850.
[70] J. Andersson, K.N. Ekdahl, J.D. Lambris, B. Nilsson, Biomaterials 26 (2005) 1477–1485.
[71] S. Yorulmaz, S.R. Tabaei, M. Kim, J. Seo, W. Hunziker, J. Szebeni, N.-J. Cho, Eur. J. Nanomed. 7 (2015) 245–255.
[72] S. Yorulmaz, J.A. Jackman, W. Hunziker, N.-J. Cho, Biomacromolecules 16 (2015) 3594–3602.
[73] B.J. Janssen, A. Christodoulidou, A. McCarthy, J.D. Lambris, P. Gros, Nature 444 (2006) 213–216.
[74] B.J. Janssen, E.G. Huizinga, H.C. Raaijmakers, A. Roos, M.R. Daha, K. Nilsson-Ekdahl, B. Nilsson, P. Gros, Nature 437 (2005) 505–511.
[75] D.T. Fearon, K.F. Austen, J. Exp. Med. 142 (1975) 856–863.
[76] M. Mousli, T. Hugli, Y. Landry, C. Bronner, J. Immunol. 148 (1992) 2456–2461.
[77] T.E. Hugli, J. Biol. Chem. 250 (1975) 8293–8301.
[78] C. Smith, M. Pangburn, C. Vogel, H. Müller-Eberhard, J. Biol. Chem. 259 (1984) 4582–4588.
[79] C. Cortes, J.A. Ohtola, G. Saggu, V.P. Ferreira, Front. Immunol. 3 (2012) 3389.
[80] M.K. Pangburn, J. Immunol. 142 (1989) 202–207.
[81] G. Sauerbrey, Zeitschrift für physik 155 (1959) 206–222.
[82] S.R. Tabaei, J.-H. Choi, G. Haw Zan, V.P. Zhdanov, N.-J. Cho, Langmuir 30 (2014) 10363–10373.
[83] S.R. Tabaei, J.A. Jackman, S.-O. Kim, V.P. Zhdanov, N.-J. Cho, Langmuir 31 (2015) 3125–3134.
[84] S.R. Tabaei, S. Vafaei, N.-J. Cho, Phys. Chem. Chem. Phys. 17 (2015) 11546–11552.
[85] K. Glasmästar, C. Larsson, F. Höök, B. Kasemo, J. Colloid Interface Sci. 246 (2002) 40–47.
[86] V. Zhdanov, B. Kasemo, Proteins: Struct. Funct. Bioinf. 30 (1998) 177–182.
[87] M. Alcorlo, A. López-Perrote, S. Delgado, H. Yébenes, M. Subías, C. Rodríguez-Gallego, S. Rodríguez de Córdoba, O. Llorca, FEBS J. 282 (2015) 3883–3891.
[88] V.P. Ferreira, C. Cortes, M.K. Pangburn, Immunobiology 215 (2010) 932–940.